ChemComm

Redox-Active Ligand Promoted Electrophile Addition at Cobalt

Journal:	*ChemComm*
Manuscript ID	CC-COM-09-2023-004869.R1
Article Type:	Communication

COMMUNICATION

Redox-Active Ligand Promoted Electrophile Addition at Cobalt

Minzhu Zou [a] and Kate M. Waldie *[a]

Received 00th January 20xx,
Accepted 00th January 20xx

DOI: 10.1039/x0xx00000x

The reactivity of an electron-rich cobalt complex bearing an *o*-phenylenediamide ligand with electrophilic CF_3^+ and F^+ sources is reported. These reactions lead to generation of the Co(III)–CF_3 or Co(III)–F complex, promoted by redox-active ligand-to-substrate two-electron transfer. The rate of trifluoromethyl addition at cobalt correlates with the potential difference between the cobalt complex and the CF_3^+ source. We present initial demonstrations of radical trifluoromethylation and nucleophilic fluorination of organic substrates, setting the stage for the development of electrocatalytic pathways for these bond-forming reactions.

Achieving control over multielectron redox processes is key to the development of selective catalytic methods using transition metal complexes for many organic transformations. While traditional ligands typically serve as spectators during electron transfer, redox-active ligands possess multiple accessible redox states and can store and release electrons to facilitate bond-breaking or bond-forming reactions, particularly at first-row metal complexes.[1] Indeed, several studies have demonstrated the unique roles of redox-active ligands for promoting multielectron reactivity with organic substrates at first-row metal centres through ligand-mediated electron transfer.[2] However, these examples largely feature complexes that exhibit distinct $1e^-$ electrochemical processes, in contrast to the $2e^-$ behaviour associated with the noble metals.[3] The ability to access $2e^-$ processes at first-row metal complexes may provide new opportunities for catalysis.

A limited number of first-row metal complexes bearing redox-active ligands exhibit a $2e^-$ redox couple,[4,5] for which a change in coordination geometry is often required to favour potential inversion[6] and access the multielectron pathway.

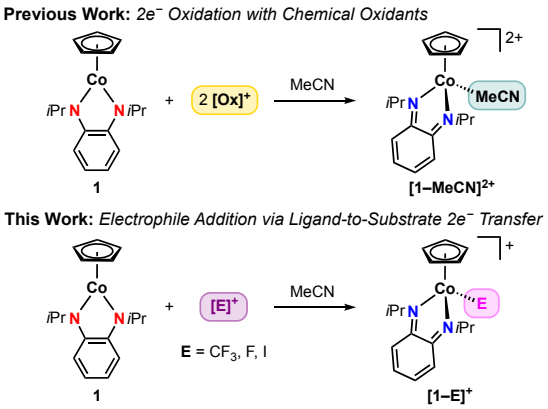

Scheme 1 Reaction of **1** with chemical oxidants[5] and electrophilic reagents promoted by ligand-based redox activity.

Among these examples, we recently reported a series of cobalt complexes based on the redox-active *o*-phenylenediamide ligand (opda).[5] By cyclic voltammetry (CV), the isopropyl derivative, complex **1**, was shown to undergo a reversible $2e^-$ oxidation at –0.17 V vs. $Fc^{+/0}$ in MeCN, yielding the dicationic complex **[1–MeCN]$^{2+}$** in which the opda ligand has been fully oxidized to the benzoquinonediimine form (bqdi; Scheme 1). This $2e^-$ oxidation can be achieved electrochemically or by treatment of **1** with a chemical oxidant. Seeking to harness this multi-electron behaviour for bond forming reactions, we demonstrate here that **1** reacts with select electrophiles to generate the monocationic species **[1–E]$^+$**, where the electrons for Co–E bond formation are derived from oxidation of the opda ligand.

The reaction of **1** with the Umemoto's reagent[7] $[DBT–CF_3]^+$ in MeCN proceeds at 25 °C to yield **2** as a deep red solid in quantitative yield (Fig. 1a). The incorporation of a CF_3 group in the product is supported by high-resolution mass spectrometry, which shows a signal corresponding to the monocation **2** (Fig. S30a). Similar to **[1–MeCN]$^{2+}$**, **2** is diamagnetic. ^{1}H NMR analysis

[a] Department of Chemistry and Chemical Biology, Rutgers, The State University of New Jersey, 123 Bevier Road, Piscataway, New Jersey 08854, USA. E–mail: kate.waldie@rutgers.edu

† Electronic Supplementary Information (ESI) available: Experimental procedures, NMR, UV-vis, Mass, and EPR spectra, CV data, and computational details. CCDC 2286968-2286970. See DOI: 10.1039/x0xx00000x

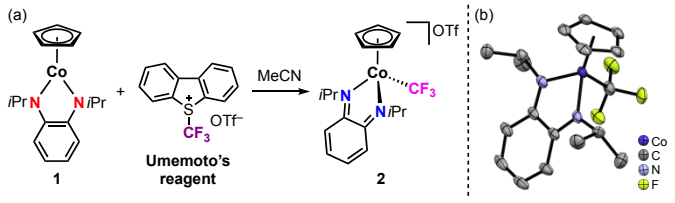

Fig. 1 (a) Synthesis of **2** via reaction of **1** with the Umemoto's reagent. (b) X-ray structure of **2** at 50% probability ellipsoids. Hydrogen atoms, co-crystallized solvent, and triflate counterion (OTf^-) are omitted for clarity.

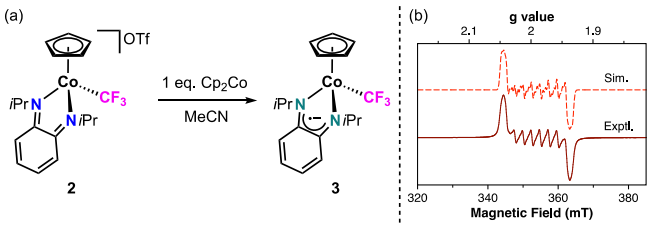

Fig. 2 (a) Synthesis of **3** via chemical reduction of **2**. (b) Experimental (solid trace) and simulated (dashed red) EPR spectra of **3** in toluene at room temperature. g_{iso} = 1.9906. A(^{14}N) = 20.7 MHz, A(^{14}N') = 18.7 MHz, A(^{59}Co) = 66.7 MHz. Linewidth = 0.85 mT.

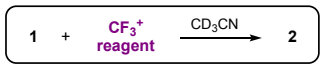

CF_3^+ Reagent	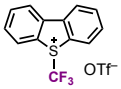 [DBT–CF_3]$^+$	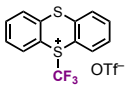 [Thi–CF_3]$^+$	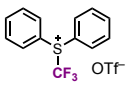 [Ph_2S–CF_3]$^+$
$E_{p,c}(CF_3^+)$ (vs. $Fc^{+/0}$)	-0.65 V	-0.85 V	-1.07 V
ΔE (V)	0.48 V	0.68 V	0.90 V
Conversion ≥85%	< 5 min	24 h	7 d

Fig. 3 Reactivity of **1** with electrophilic CF_3^+ reagents. Reaction time correlates with ΔE, the difference between $E_{1/2}$(**1**) and the reduction peak potential of the CF_3^+ reagent, $E_{p,c}(CF_3^+)$.

reveals that the cyclopentadienyl (Cp) signal in **2** (δ 5.78 ppm) is shifted downfield compared to **1** (δ 4.98 ppm), consistent with an increased charge of the complex. The ^{19}F NMR spectrum shows a singlet at δ -7.03 ppm (Fig. S6), which is assigned to the trifluoromethyl ligand coordinated to cobalt.[8] The crystal structure of **2** confirms the Co–CF_3 bond formation (Fig. 1b). The N–$C_{phenylene}$ bond length in **2** is 1.311(5) Å, comparable to the ligand backbone in **[1–MeCN]$^{2+}$**.[5] Overall, **2** is formulated as a coordinatively saturated Co(III) centre with a fully oxidized bqdi ligand and anionic trifluoromethyl ligand; thus, the formation of **2** involves formal ligand-to-substrate redox transfer.

CV studies of **2** in 0.1 M [^{n}Bu$_4$N][PF_6] in MeCN show a reversible 1e$^-$ reduction at –0.62 V vs. $Fc^{+/0}$ (Fig. S27), suggesting that the reduction product may be isolable. Indeed, chemical reduction of **2** with 1 eq cobaltocene yields the neutral complex **3** in 91% yield (Fig. 2a). The magnetic moment of **3**, obtained by Evans method in CD_3CN at 25 °C, is 1.86 μB, consistent with the presence of one unpaired electron (S = ½). In the crystal structure (Fig. S2), there is slight shortening of the Co–CF_3 bond and elongation (ca. 0.03 Å) of the N–$C_{phenylene}$ bonds compared to **2** – the latter suggests a ligand-based reduction. This proposal is further supported by EPR analysis of **3** recorded in toluene at room temperature and 77 K (Fig. 2b and S31). The EPR parameters are characteristic of a ligand-centred radical with relatively small magnitude hyperfine couplings to ^{59}Co. Density functional theory (DFT) calculations also support this assignment, where the Mulliken spin density is primarily localized on the ligand (Fig. S34). Thus, the electronic structure of **3** is best described as a Co(III) centre with a semi-benzoquinonediimine (s-bqdi) radical anion ligand. This result is in stark contrast to **[1–MeCN]$^+$** in which the radical spin density was calculated by DFT to be mainly centred on cobalt.[5]

The 1e$^-$ reduction of **2** can also be monitored by UV-vis spectroelectrochemistry (Fig. S26b). The electronic spectrum of **2** shows two absorptions in the visible range at 409 and 518 nm, with no absorption features beyond 700 nm. Upon reduction, new bands appear in the near-IR region at 753, 844, and 961 nm. Similar features have been reported for related complexes with ligand-centred radical(s).[4c, 9] A second 1e$^-$ reduction for **2** is observed by CV at –1.55 V vs. $Fc^{+/0}$ (Fig. S28). This process is chemically irreversible and leads to new oxidative features on the reverse scan, indicating that the anionic species undergoes further reaction that may involve the CF_3 ligand. Studies to probe this reactivity are currently ongoing in our group.

Notably, **2** can also be generated via treatment of **1** with other electrophilic trifluoromethylation reagents (Fig. 3). The rate of this reaction trends with the reduction peak potential ($E_{p,c}$) of the electrophile, where reagents with more positive $E_{p,c}$ values exhibit faster reactivity. For example, the reaction of **1** and [Thi–CF_3]$^+$ takes 24 h to reach 85% conversion, while the same reaction with [Ph_2S–CF_3]$^+$ requires 7 days.

The $E_{p,c}$ value of [DBT–CF_3]$^+$ is –0.87 V vs $Fc^{+/0}$ in MeCN, which is the most positive reduction potential among the CF_3^+ reagents examined here (Fig. S29). However, this value is still 0.48 V more negative than the reversible 2e$^-$ oxidation potential of **1**. Thus, the trifluoromethylation reaction at cobalt is likely driven by formation of the Co–CF_3 bond, which compensates for the unfavourable potential difference for outer-sphere 2e$^-$ transfer.

Further insights into the mechanism of this reaction were explored using TEMPO (2,2,6,6-tetramethylpiperidine-*N*-oxyl radical). No reaction is observed when TEMPO is added to a solution of either **2** or [DBT–CF_3]$^+$. However, when a solution of **1** in CD_3CN is treated with 1 eq [DBT–CF_3]$^+$ and 1 eq TEMPO at 25 °C, TEMPO–CF_3 is obtained in 73% yield within 10 min (Scheme 2a), based on its diagnostic ^{19}F NMR signal at –55.04 ppm (Fig. S13).[10] The formation of TEMPO–CF_3 implicates the involvement of a short-lived trifluoromethyl radical ($CF_3^\bullet$) in the reaction of **1** and [DBT–CF_3]$^+$, which may form by an initial single electron transfer between the opda ligand and the CF_3^+ source. In the absence of TEMPO, the resulting $CF_3^\bullet$ radical is likely rapidly reduced with concomitant Co–CF_3 bond formation to yield **2**. However, even in the presence of TEMPO, NMR signals for **2** are also observed (Figure S12-S13), indicating that the pathway leading to **2** is competitive with TEMPO–CF_3 formation. The proposed $CF_3^\bullet$ radical mechanism is also supported by the observation of **[1–MeCN]$^{2+}$** in the reaction mixture when **1** is

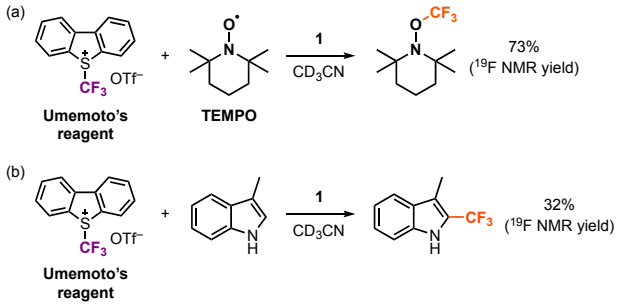

Scheme 2 Stoichiometric CF_3 radical addition to (a) TEMPO, and (b) 3-methyl-1*H*-indole.

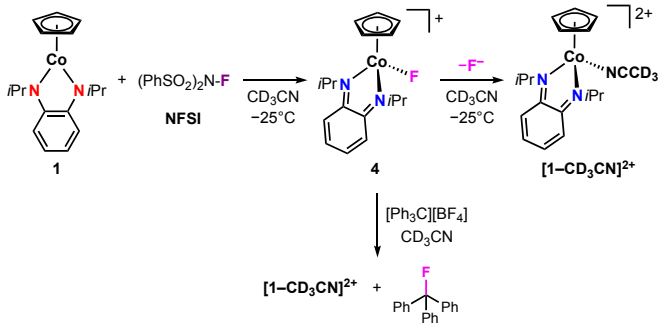

Scheme 3 Reaction of **1** with NFSI to generate **4**. The fluoride ligand is gradually displaced by CD_3CN solvent, or the fluoride can be trapped by addition of $[Ph_3C][BF_4]$.

treated with 2 eq TEMPO and 2 eq $[DBT–CF_3]^+$, where **[1–MeCN]$^{2+}$** may be generated from the disproportionation of **[1]$^+$**.[5]

To probe the possibility of radical trifluoromethylation of other organic substrates, we tested the reactivity of **1** in the presence of $[DBT–CF_3]^+$ and 3-methyl-1*H*-indole at 25 °C. Indeed, the formation of 3-methyl-2-(trifluoromethyl)-1*H*-indole was observed by ^{1}H and ^{19}F NMR within 20 min (Fig. S14-S15), confirming trifluoromethyl radical addition (Scheme 2b). With this successful initial demonstration of trifluoromethylation, further studies to optimize this reactivity and explore a larger substrate scope are underway.

We note that our cobalt system resembles the reactivity of a Cu(II) bis(*o*-iminosemiquinonate) complex $[Cu(L^{\bullet}_{SQ})_2]$ with $[DBT–CF_3]^+$.[11] In this case, the trifluoromethylation reaction at copper proceeds overnight with 1e$^-$ oxidation of each ligand to the iminobenzoquinone form. These ligand oxidations occur at well-separated, sequential 1e$^-$ redox potentials (E_1 = –0.26 V, E_2 = +0.37 V vs. $Fc^{+/0}$ in CH_2Cl_2),[4c] compared to the 2e$^-$ oxidation of **1** at –0.17 V. While E_1 for $[Cu(L^{\bullet}_{SQ})_2]$ is more negative than the oxidation potential of **1**, the potential difference between E_2 and $E_{p,c}([DBT–CF_3]^+)$ is greater (ΔE = 1.02 V, compared to only 0.48 V for **1**). Thus, the multi-electron behaviour of **1** may promote more rapid reactivity at cobalt, thanks to the overall more favourable ligand-to-substrate 2e$^-$ transfer.

We have also expanded the scope of the reactivity of **1** with other electrophilic reagents, including NFSI (*N*-fluorodibenzenesulfonimide, $E_{p,c}$ = –1.16 V vs. $Fc^{+/0}$ in MeCN, Fig. S29),[12] NIS (*N*-iodosuccinimide), and iodine. Treatment of **1** with 1 eq NFSI in CD_3CN at room temperature results in a rapid reaction, yielding **[1–CD$_3$CN]$^{2+}$** as the only cobalt species by NMR analysis. Repeating this experiment at –25 °C reveals a broad ^{19}F NMR signal at –654 ppm, which is assigned as the fluoride ligand in **4** by comparison with other reported [Co–F] complexes (Scheme 3).[8] Complex **4** is stable at –25 °C in CD_3CN for at least 3 h, but the fluoride ligand is gradually displaced by solvent to generate **[1–CD$_3$CN]$^{2+}$** (Fig. S18). While we have been unable to characterize **4** further, we propose that Co–F bond formation likewise proceeds with formal oxidation of the opda ligand. This reactivity is mirrored by the reaction of **1** with *N*-iodosuccinimide or iodine, yielding **5** which can be isolated due to its greater stability. The crystal structure of **5** shows similar structural metrics as **2** (Fig. S3), with N–$C_{phenylene}$ bond lengths of 1.303(5) and 1.316(5) Å. Complex **5** is stable in THF solution, but an equilibrium mixture of **5** and **[1–MeCN]$^{2+}$** is established in MeCN within ca. 1 h (Fig. S22).

The facile release of fluoride from **4** prompted us to explore new avenues for delivering nucleophilic fluoride to electrophilic substrates, starting with an electrophilic F^+ source. For an initial demonstration, we selected the trityl cation as the substate partner. Treatment of freshly prepared **4** in cold CD_3CN with trityl tetrafluoroborate leads to formation of trityl fluoride, as evidenced by its ^{19}F NMR signal at –125.32 ppm (Fig. S25).[13] At the same time, ^{1}H NMR signals for **[1–CD$_3$CN]$^{2+}$** are also observed. Thus, this reaction demonstrates the umpolung of the initial F^+ source and the stoichiometric delivery of F^- to an electrophile. In principle, the subsequent reduction of **[1–CD$_3$CN]$^{2+}$** would regenerate **1**, thus establishing a cycle for the electrocatalytic fluorination of organic substrates. We are currently working to identify electrophile partners that are compatible with this scheme.

In summary, we have shown that complex **1** undergoes facile reactivity with electrophiles to yield a new Co–E bond, where the electron source originates from the redox-active ligand while bond formation is centred at the cobalt. The reaction rate between **1** and CF_3^+ sources trends with the reduction potential of the electrophile, where reagents with more positive reduction potentials exhibit faster reactivity. Initial mechanistic studies into this reactivity suggest a $CF_3^{\bullet}$ radical pathway, which can be intercepted with TEMPO or 3-methyl-1*H*-indole. The reaction of **1** with a F^+ electrophile results in formal umpolung of the fluorine, delivering nucleophilic fluoride. These proof-of-principle studies show the potential of **1** for promoting radical trifluoromethylation[14] and nucleophilic fluorination[15] of organic substrates. The development of electrocatalytic protocols for these reactions is currently underway.

This work was supported by the ACS Petroleum Research Fund (65171-DNI3) and Rutgers, The State University of New Jersey. The Rigaku SYNERGY-S X-ray diffractometer was partially funded by an NSF MRI Award (CHE-2117792). We acknowledge the Office of Advanced Research Computing (OARC) at Rutgers University for providing access to the Amarel Cluster and associated research computing resources. We thank Dr. Alexei M. Tyryshkin for assistance with EPR analysis, and Dr. Thomas J. Emge for assistance with crystal structure refinements.

Conflicts of interest

There are no conflicts to declare.

References

1 (a) P. J. Chirik and K. Wieghardt, *Science*, 2010, **327**, 794; (b) P. J. Chirik, *Inorg. Chem.*, 2011, **50**, 9737; (c) W. Kaim, *Inorg. Chem.*, 2011, **50**, 9752; (d) O. R. Luca and R. H. Crabtree, *Chem. Soc. Rev.*, 2013, **42**, 1440.

2 (a) V. Lyaskovskyy and B. de Bruin, *ACS Catal.*, 2012, **2**, 270; (b) D. L. J. Broere, R. Plessius and J. I. van der Vlugt, *Chem. Soc. Rev.*, 2015, **44**, 6886; (c) J. I. van der Vlugt, in *Pincer Compounds: Chemistry and Applications*, ed. D. Morales-Morales, Elsevier, 2018, pp. 599; (d) K. Singh, A. Kundu and D. Adhikari, *ACS Catal.*, 2022, **12**, 13075; (e) A. L. Smith, K. I. Hardcastle and J. D. Soper, *J. Am. Chem. Soc.*, 2010, **132**, 14358; (f) M. van der Meer, Y. Rechkemmer, I. Peremykin, S. Hohloch, J. van Slageren and B. Sarkar, *Chem. Commun.*, 2014, **50**, 11104.

3 K. P. Kepp, *ChemPhysChem*, 2020, **21**, 360.

4 (a) S. A. Richert, P. K. S. Tsang and D. T. Sawyer, *Inorg. Chem.*, 1989, **28**, 2471; (b) P. N. Bartlett and V. Eastwick-Field, *Electrochim. Acta*, 1993, **38**, 2515; (c) P. Chaudhuri, C. N. Verani, E. Bill, E. Bothe, T. Weyhermüller and K. Wieghardt, *J. Am. Chem. Soc.*, 2001, **123**, 2213; (d) E. Bill, E. Bothe, P. Chaudhuri, K. Chlopek, D. Herebian, S. Kokatam, K. Ray, T. Weyhermüller, F. Neese and K. Wieghardt, *Chem. Eur. J.*, 2005, **11**, 204; (e) K. Chlopek, E. Bothe, F. Neese, T. Weyhermuller and K. Wieghardt, *Inorg. Chem.*, 2006, **45**, 6298; (f) C. Mukherjee, T. Weyhermuller, E. Bothe and P. Chaudhuri, *Inorg. Chem.*, 2008, **47**, 11620; (g) S. K. Sharma, P. S. May, M. B. Jones, S. Lense, K. I. Hardcastle and C. E. MacBeth, *Chem. Commun.*, 2011, **47**, 1827; (h) P. Ghosh, S. Samanta, S. K. Roy, S. Joy, T. Krämer, J. E. McGrady and S. Goswami, *Inorg. Chem.*, 2013, **52**, 14040; (i) D. Sengupta, P. Ghosh, T. Chatterjee, H. Datta, N. D. Paul and S. Goswami, *Inorg. Chem.*, 2014, **53**, 12002; (j) M. D. Sampson, A. D. Nguyen, K. A. Grice, C. E. Moore, A. L. Rheingold and C. P. Kubiak, *J. Am. Chem. Soc.*, 2014, **136**, 5460; (k) K. M. Waldie, S. Ramakrishnan, S.-K. Kim, J. K. Maclaren, C. E. D. Chidsey and R. M. Waymouth, *J. Am. Chem. Soc.*, 2017, **139**, 4540; (l) B. D. Matson, E. A. McLoughlin, K. C. Armstrong, R. M. Waymouth and R. Sarangi, *Inorg. Chem.*, 2019, **58**, 7453; (m) C. S. Richburg and B. H. Farnum, *Inorg. Chem.*, 2019, **58**, 15371; (n) M. M. R. Mazumder, A. Burton, C. S. Richburg, S. Saha, B. Cronin, E. Duin and B. H. Farnum, *Inorg. Chem.*, 2021, **60**, 13388; (o) H. Bamberger, U. Albold, J. Dubnická Midlíková, C.-Y. Su, N. Deibel, D. Hunger, P. P. Hallmen, P. Neugebauer, J. Beerhues, S. Demeshko, F. Meyer, B. Sarkar and J. van Slageren, *Inorg. Chem.*, 2021, **60**, 2953.

5 M. Zou, T. J. Emge and K. M. Waldie, *Inorg. Chem.*, 2023, **62**, 10397.

6 D. H. Evans, *Chem. Rev.*, 2008, **108**, 2113.

7 (a) T. Umemoto and S. Ishihara, *Tetrahedron Lett.*, 1990, **31**, 3579; (b) T. Umemoto and S. Ishihara, *J. Am. Chem. Soc.*, 1993, **115**, 2156.

8 M. C. Leclerc, J. M. Bayne, G. M. Lee, S. I. Gorelsky, M. Vasiliu, I. Korobkov, D. J. Harrison, D. A. Dixon and R. T. Baker, *J. Am. Chem. Soc.*, 2015, **137**, 16064.

9 S. Sobottka, M. B. van der Meer, E. Glais, U. Albold, S. Suhr, C.-Y. Su and B. Sarkar, *Dalton Trans.*, 2019, **48**, 13931.

10 (a) X. Wang, Y. Ye, S. Zhang, J. Feng, Y. Xu, Y. Zhang and J. Wang, *J. Am. Chem. Soc.*, 2011, **133**, 16410; (b) J. Jacquet, S. Blanchard, E. Derat, M. Desage-El Murr and L. Fensterbank, *Chem. Sci.*, 2016, **7**, 2030.

11 J. Jacquet, E. Salanouve, M. Orio, H. Vezin, S. Blanchard, E. Derat, M. Desage-El Murr and L. Fensterbank, *Chem. Commun.*, 2014, **50**, 10394.

12 (a) A. G. Gilicinski, G. P. Pez, R. G. Syvret and G. S. Lal, *J. Fluorine Chem.*, 1992, **59**, 157; (b) J. R. Aranzaes, M.-C. Daniel and D. Astruc, *Can. J. Chem.*, 2006, **84**, 288.

13 G. W. Farley, M. A. Siegler and D. P. Goldberg, *Inorg. Chem.*, 2021, **60**, 17288.

14 (a) H. Xiao, Z. Zhang, Y. Fang, L. Zhu and C. Li, *Chem. Soc. Rev.*, 2021, **50**, 6308; (b) D. Mandal, S. Maji, T. Pal, S. K. Sinha and D. Maiti, *Chem. Commun.*, 2022, **58**, 10442.

15 (a) R. Szpera, D. F. J. Moseley, L. B. Smith, A. J. Sterling and V. Gouverneur, *Angew. Chem. Int. Ed.*, 2019, **58**, 14824; (b) I. N.-M. Leibler, S. S. Gandhi, M. A. Tekle-Smith and A. G. Doyle, *J. Am. Chem. Soc.*, 2023, **145**, 9928.